

Article

Influence of the Oxygen Surface Functionalities Introduced by Electrochemical Treatment on the Behavior of Graphite Felts as Electrodes in VRFBs

Laura García-Alcalde , Alejandro Concheso , Victoria G. Rocha, Clara Blanco, Ricardo Santamaría * and Zoraida González *

Instituto de Ciencia y Tecnología del Carbono (INCAR), CSIC, Francisco Pintado Fe 26, 33011 Oviedo, Spain

* Correspondence: riqui@incar.csic.es (R.S.); zoraidag@incar.csic.es (Z.G.)

Abstract: Graphite felts act as electrodes in VRFBs thanks to their properties such as chemical strength and electrical conductivity or 3D-structure. However, there are significant drawbacks to be overcome, such as their low wettability, sluggish kinetic reversibility and electroactivity towards faradaic processes related to vanadium electroactive species. As a consequence, it is key to alter the fibres to enhance their electrochemical performance during battery operation. Most of the previously reported modifications have been focused on incorporating surface oxygenated functional groups, even though the role of those groups on the electrocatalytic activity towards vanadium faradaic processes is still not clear. Aiming to gain knowledge on this issue, this work investigates the influence of electro-oxidation and electro-reduction treatments, performed in different acidic media (H_2SO_4 or HNO_3 solutions), on their subsequent electrochemical response towards VO^{2+}/VO_2^+ and V^{3+}/V^{2+} faradaic processes. The chemical and electrochemical properties of the modified felts were analyzed to understand two key parameters that affect the vanadium reaction catalysis: the depth and oxidation degree of the fibres. A treatment with HNO_3 , a strong oxidizing agent, leads to a deep oxidation of the fibre and the development of a high density of oxygenated functional groups, mainly C=O, which hinder the redox reactions of vanadium, especially for the faradaic reactions from the catholyte.

Keywords: graphite felts; electrochemical treatments in acidic media; depth and oxidation degree; electrocatalytic activity; vanadium redox processes



Citation: García-Alcalde, L.; Concheso, A.; Rocha, V.G.; Blanco, C.; Santamaría, R.; González, Z. Influence of the Oxygen Surface Functionalities Introduced by Electrochemical Treatment on the Behavior of Graphite Felts as Electrodes in VRFBs. *Batteries* **2022**, *8*, 281. <https://doi.org/10.3390/batteries8120281>

Academic Editors: Zexiang Shen and Linfei Lai

Received: 31 October 2022

Accepted: 8 December 2022

Published: 10 December 2022

Publisher's Note: MDPI stays neutral with regard to jurisdictional claims in published maps and institutional affiliations.



Copyright: © 2022 by the authors. Licensee MDPI, Basel, Switzerland. This article is an open access article distributed under the terms and conditions of the Creative Commons Attribution (CC BY) license (<https://creativecommons.org/licenses/by/4.0/>).

1. Introduction

Global energy demand is increasing by leaps and bounds as a result of population and economic growth. As a result, in the last decades the massive use of fossil fuels has accelerated the climate change with disastrous consequences worldwide. Because of this, the transformation of the current energy model towards a greener, more sustainable and resilient scenario becomes a priority [1]. In this context, the transition to a model based on renewable resources is essential to limit dependence on non-renewable fuel sources. However, this ambitious but necessary goal implies the design and development of reliable and flexible storage systems able to overcome the problems associated with the intermittent supply of electricity, thus guaranteeing a balance between supply and demand [2]. Within the wide variety of available energy storage technologies, electrochemical devices, and in particular redox flow batteries (RFBs), have gained in interest when considering energy storage in stationary applications. The possibility of decoupling their power and energy (being the first one determined by the electrode area and efficiency, which can be related to the number of cells, and the second one dependent on the nature, molarity and volume of the electrolytes) provides them with such attractive features as unlimited capacity, high efficiency, and flexible and safe design for an extensive variety of applications, as well as longer useful life, which facilitates their amortization despite the high initial investment [3].

Similar to other secondary batteries, RFBs are electrochemical devices with two electrodes, with the uniqueness of using two electrolytic solutions stored in two independent and outer containers from which they flow through the electrochemical cell, which contains an ion selective membrane to separate the two half cells [4]. Among the various possible chemistries, batteries based on vanadium species (VRFBs) are the most attractive ones mainly in terms of design and operation. Although VRFB is not cheap due to electrolyte cost, it displays better reversibility and higher kinetics than, for example, Fe-based RFBs [5]. Moreover, it can avoid the dendrite problem in Zn-based RFBs caused by the undesired deposition of Zn in the anode [6]. In addition, the use of vanadium species in the two half-cells allows for the preventing of cross-contamination drawbacks, even though several researchers are investigating the improvement of membranes selectivity in depth [3,7]. Despite the fact that energy is not directly stored in the electrodes, they determine the proper operation of the device, as they support the faradaic processes involved in the charge and discharge of the battery. Thus, the selection of active electrode materials offering a suitable electrochemical behaviour is crucial to increasing the battery performance. Graphite felts are traditional electrodes in these devices as a consequence of the combination of several appropriate characteristics such as high electrical conductivity, large active surface area and good chemical stability [8]. Nevertheless, they exhibit sluggish kinetic and electroactivity to the faradaic processes of the vanadium species involved. Consequently, many efforts focus on improving their electrochemical performance following different routes such as heteroatoms incorporation, oxidation treatments or deposition of metallic nanoparticles or different carbon nanomaterials [9,10]. Most of the previously reported studies agree on the fundamental role that surface oxygenated functional groups (OFGs_x) play on battery performance. However, rather contradictory results are published about the role of these groups on the electroactivity of vanadium species [11].

Skyllas-Kazacos was one of the first scientists who emphasized the relevant role of OFGs on electrode kinetics in VRFBs. In her work with Sun [12], they highlighted the positive impact of the surface oxygenated groups incorporated on the electrode hydrophilicity and on increasing its electrochemically active surface area, thus enhancing the electroactivity to vanadium reactions. Moreover, they have further investigated chemical modification of these felts using oxidizing agents such as sulfuric acid, nitric acid and mixtures of both [13], showing a better cell operation due to the oxidation of unsaturated bonds and their conversion into OFGs on a graphite felt surface and to the removal of impurities hampering electron transfer processes. They also pointed out that the electrodes increased electrical resistance after modification with HNO₃ or H₂SO₄:HNO₃ (3:1) in comparison with those only treated with H₂SO₄, but they do not provide an explanation about the surface chemistry developed after each acidic treatment or its influence on the electrode materials' electroactivity.

Since then, several studies have been published looking at improving the electrochemical response towards vanadium reactions through the modification of the surface chemistry of graphite felt (GF) electrodes. Thus, Kim et al. [14] presented a comparative study on the effect of different oxidation treatments on the surface morphology and on the electrochemical behavior of GF electrodes, reporting that the quantity and nature of oxygenated groups developed significantly affect the suitable development of the redox processes of interest. Similarly, Dixon et al. [15] reported the influence of oxygen plasma treatment on the performance of GFs of different natures. The fibres presented an improved redox activity towards the anolyte faradaic processes in contrast with electrochemical activity towards VO²⁺/VO₂⁺, which showed a clear worsening of the unmodified felt performance. Wu et al. [16] explored the benefits of treating graphite felts under microwave heating, concluding that more hydrophilic groups were introduced on felt fibre defects, also increasing their activity to vanadium redox reactions, results that are also supported by Cho et al. [17].

In recent years, carbon nanomaterials (e.g., graphene oxides or carbon nanowalls) with high oxygen content have been used as modifiers to improve the electrochemi-

cal behavior of traditional fibre electrodes. In this sense, Li et al. [18] wrapped fibres with graphene nanowalls, creating 3D structures enriched in oxygen containing functional groups, thus providing a network of reaction sites for $\text{VO}^{2+}/\text{VO}_2^+$ redox reactions. Etienne et al. [19] demonstrated how the modification of graphite felts by means of depositing films of MWCNTs significantly improved battery operation parameters.

Electrochemical treatments represent an attractive option for generating OFGs in the surface of graphite felts due to the possibility of performing electric potential-driven activation of the raw material directly in the assembled cell. In this regard, Li et al. studied electrooxidized graphite felts as electrodes in VRFBs [20], discussing the impact of oxygen groups (mainly-COOH) available on the overall rate of vanadium redox reactions [21]. Zhang et al. [22] prepared graphite felts with a high content of hydroxyl and carboxyl groups on their surface via electro-oxidation in sulphuric acid solution, evaluating how their oxidation degree affects the kinetics of vanadium electrochemical responses. Related to this, Wang and co-workers [23] studied the development of $\text{VO}^{2+}/\text{VO}_2^+$ reactions on graphite-based disks oxidized by following an electrochemical procedure, attributing the higher constant rate and activation energy to the higher content of OFGs. Li et al. [24] developed a controllable electrochemical modification method to obtain partially reduced graphene oxides, showing that a higher content of surface carbonyl groups significantly improved the response towards the appropriate development of vanadium reactions. More recently, Noack and co-workers [25] attributed hydroxyl groups development during the electrotreatment to $\text{VO}^{2+}/\text{VO}_2^+$ improvement, rejecting the role of carboxyl groups on the electrochemical response. Another approach has been proposed by Bourke and co-workers [26], demonstrating for different carbon electrode materials that the $\text{VO}^{2+}/\text{VO}_2^+$ reaction improved with cathodic polarized electrodes, in contrast with the $\text{V}^{3+}/\text{V}^{2+}$ reaction which is enhanced by anodic polarization. In later studies by Miller [27], different electrochemical measurements were performed on carbon fibre microelectrodes showing that anodic electrochemical procedures enhanced the kinetics of $\text{V}^{3+}/\text{V}^{2+}$ while inhibiting the corresponding to $\text{VO}^{2+}/\text{VO}_2^+$ due to a highly oxidized surface. However, cathodic treatments resulted in opposite electrochemical behaviors, due to the resultant surface chemistry being similar to the unmodified electrode, with a poor oxygen content. The positive influence of OFGs on improving $\text{V}^{3+}/\text{V}^{2+}$ redox reaction kinetics has also been noted in other published studies [28,29]. Despite the aforementioned studies, the variability of the results obtained clearly show that the role of OFGs on the catalysis of vanadium redox reactions remains an ongoing topic.

In this work we assess the impact of different electrochemical treatments on the behaviour of the resulting modified materials as supports for the development of vanadium redox reactions. Modified graphite felts have been structurally, chemically and electrochemically characterized, trying to clarify the correlation between their chemical surface characteristics and subsequent electrochemical performance as electrodes in VRFBs.

2. Results and Discussion

2.1. Impact of the Electrochemical Treatments on the Chemical Composition of the Felts

In order to elucidate the impact of the surface chemistry of the modified felts on their electrochemical behavior towards vanadium species reactions, the electrochemically modified felts in different acid media were firstly characterized by elemental microanalysis (Figure 1a and Table A1 Appendix A), also including starting GF for comparative purposes. It is expected that the electro-oxidation process in the presence of oxidizing acids leads to a progressive oxidation of some carbon sites (mainly those located in the vicinity of imperfect carbon atoms of the GF surface which are high-activity sites that readily oxidize) resulting in the presence of different oxygenated functional groups (C-OH, C=O and COOH), while evolving CO and/or CO_2 [30].

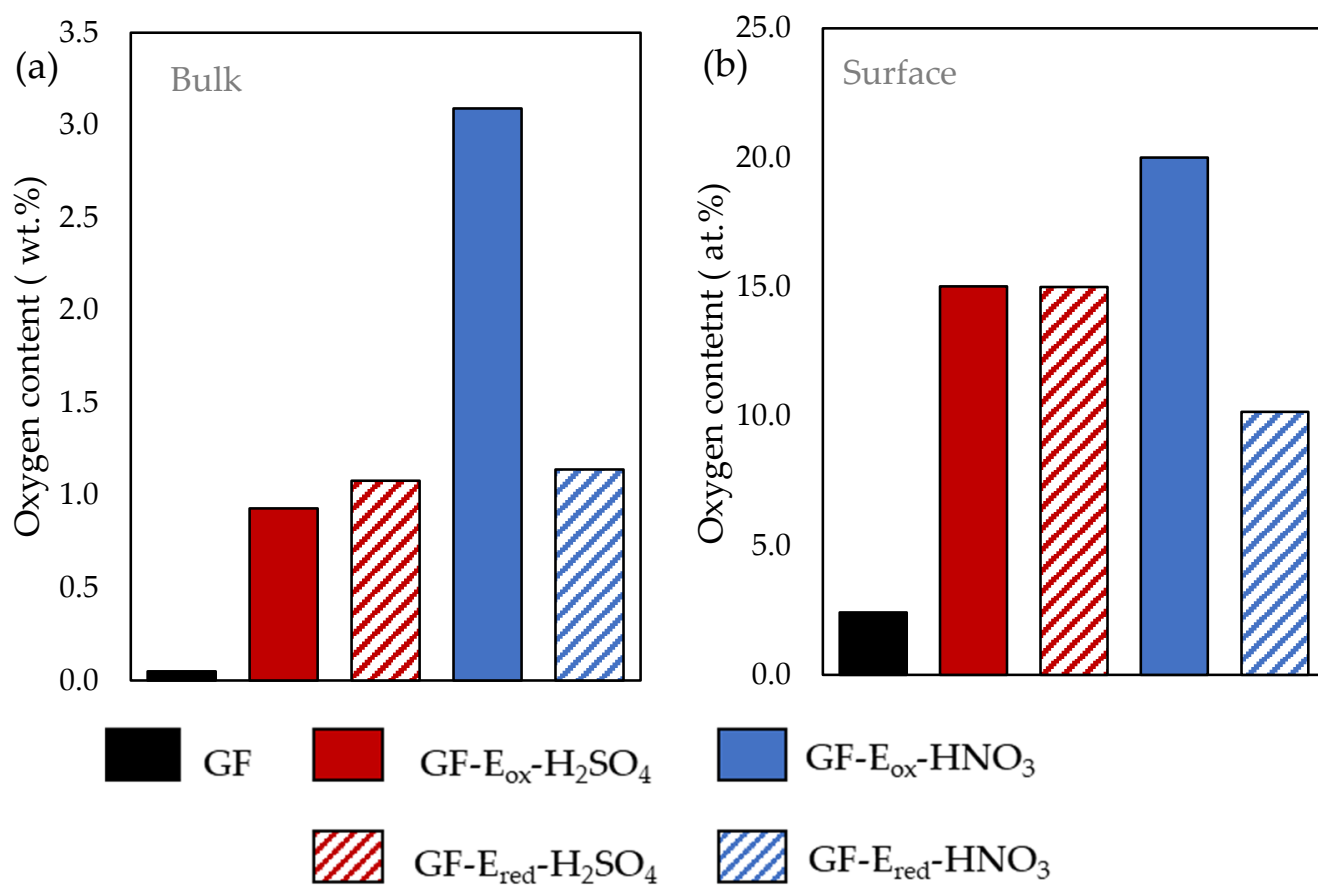


Figure 1. Bulk (a) and surface (b) oxygen content measured from micro-elemental analysis and XPS, respectively, for the different felts.

As it can be seen, the oxygen content determined by elemental analysis significantly rises from the raw material (0.05 wt.%) to those submitted to the different electrochemical procedures (Figure 1a), especially for the felt treated in the presence of nitric acid solution (3.09 wt.%). However, the oxygen functional groups introduced on GF-E_{ox}-HNO₃ seems to be less stable than those of GF-E_{ox}-H₂SO₄, which is in agreement with the marked decrease of total oxygen content of the former after the subsequent electro-reduction step.

To gain further insight onto the chemical composition of the surface of the samples, XPS analyses were carried out. The atomic surface oxygen amount (O at. %) derived from XPS survey spectra was plotted on Figure 1b, being consistent with previous elemental analysis results, showing a large content of oxygen functionalities on the modified felts in contrast with the pristine material, and emphasizing the oxygen content changes between oxidized and reduced felts treated in nitric acid. The observation of Figure 1a,b allows to infer an important difference depending on the acid media selected for the electrooxidation treatment, as felt fibres oxidized in nitric acid suffered a more aggressive attack, perhaps with the oxygen functionalities going deeper into the fibre and creating a thicker oxidized layer on them, which could negatively affect their electrochemical performance. However, such functionalities are easily removed under electro-reduction conditions.

Figure 2a,b show C1s high resolution spectra and the peaks resulting from their deconvolution, respectively, for the different GFs under study. To provide a clear comparison between different surface functional groups on the modified materials and trying to clarify their correlation with activation conditions, both the quantitative results related to the different felts and the atomic C and O percentages were summarized in Figure 3 and Table A2 Appendix A.

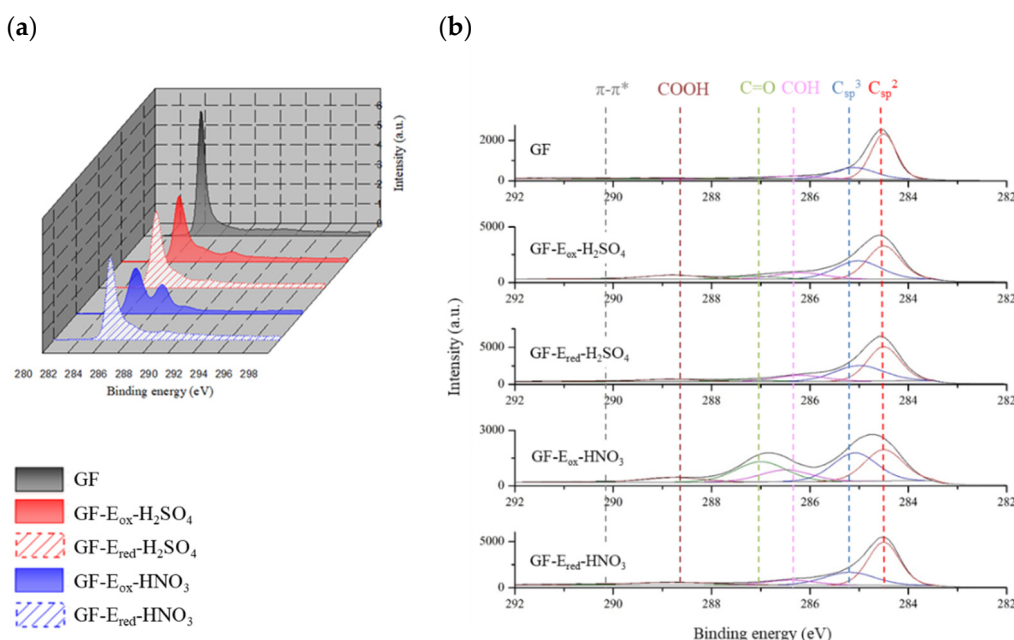


Figure 2. C1s high resolution spectra of the different felts (a) and their corresponding deconvoluted peaks (b).

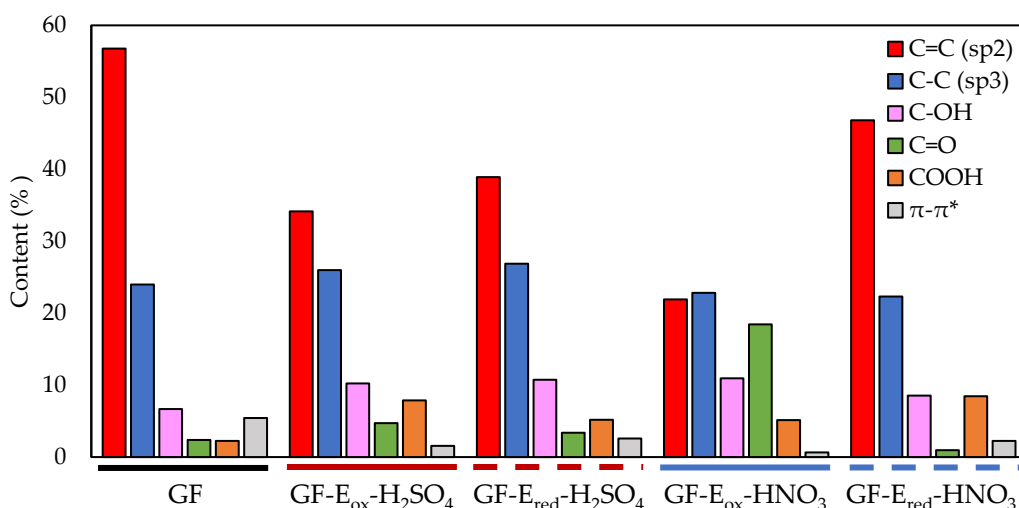


Figure 3. Percentage of the different oxygen functional groups present on the surface of tested felts.

As it can be seen in the XPS results plotted in Figure 1b and further high resolution analysis in Figure 3, GF-E_{ox}-H₂SO₄, with an enhanced surface oxygen content (15 vs. 2.4 at. % for starting GF), mainly exhibits C-OH groups (10.2%), although there is also an important amount of COOH functionalities (7.9%). In comparison, the surface oxidation is much more intense when the electrolyte is nitric acid, as the surface oxygen content reaches 20 at.%. Moreover, another remarkable result is the high content of carbonyl groups (18%), which is much higher than in the other studied samples.

A deeper data analysis of the surface chemistry of the different felts, Figure 4 presents the evolution of the oxygen functionalities after the electrochemical reduction of the previously electro-oxidized felts. The total oxygen content and the type and amount of OFGs remained practically unchanged after reduction treatment in sulphuric acid, underlining a slight increase of C_{sp}² content related with the minor reduction of C=O and COOH groups (see also Figure 3 and Table A2 Appendix A). In contrast, GF-E_{red}-HNO₃ experienced a sharp decline in the surface oxygen, with practically all carbonyl groups (and, to a lesser extent, hydroxyl groups) generated in the previous electrooxidation treatment

being drastically reduced to C=C. C_{sp^2} content increased more than 100% with respect to GF-E_{ox}-HNO₃, and the percentage of $\pi-\pi^*$ was tripled (Figure 3 and Table A2 Appendix A), thus representing a remarkable restoration of the aromatic network of the starting graphite fibre. In view of this data, oxygen functional groups introduced by sulphuric acid treatment are clearly very stable and difficult to reduce, in contrast with the ones developed in nitric acid, which are labile and easily reduced.

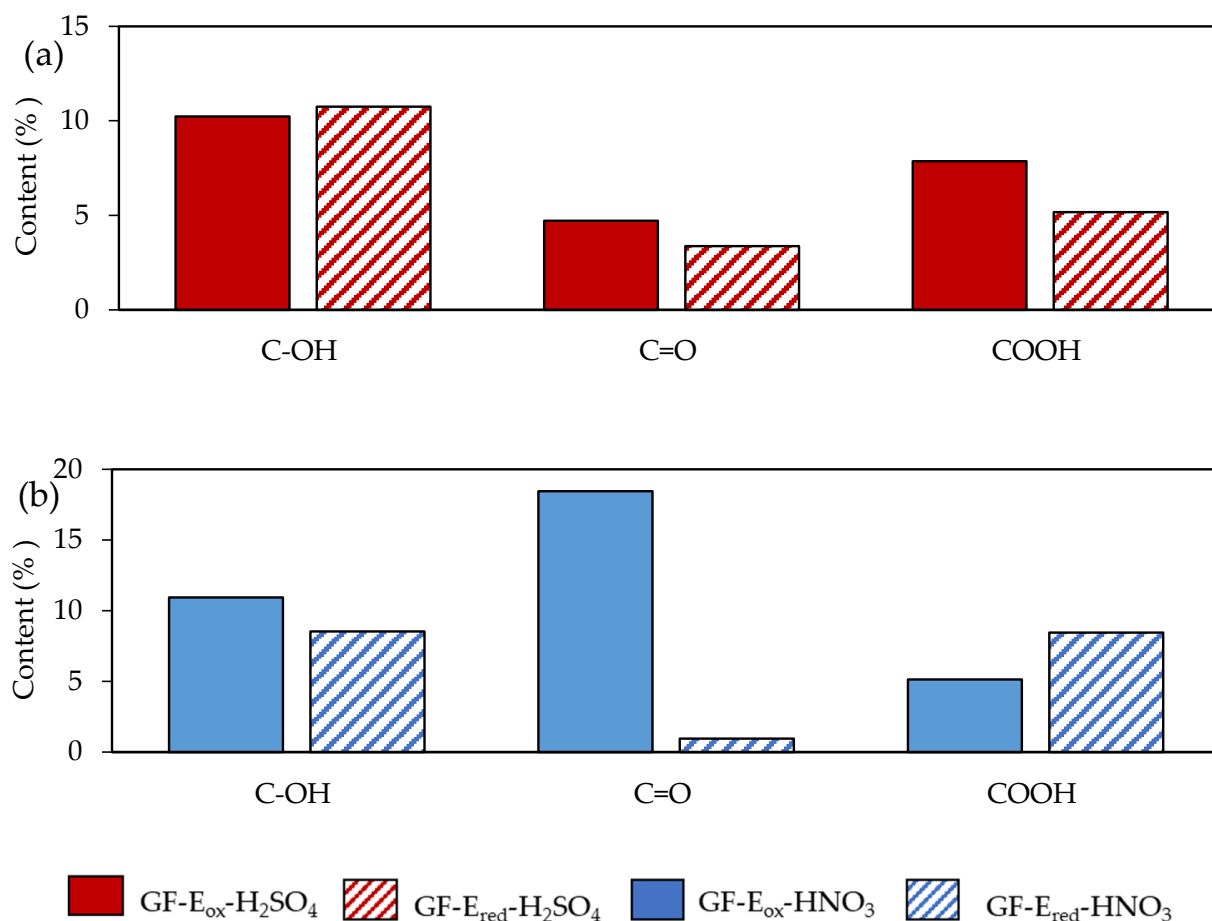


Figure 4. Evolution of the oxygen functional groups percentages determined by XPS for felts after electrochemical treatments in H₂SO₄ (a) and HNO₃ (b) media.

2.2. Electrochemical Performance of Modified Felts towards Vanadium Redox Processes

The significant differences found in the modified felts resulting from previously described electrochemical treatments should be in line with different electrochemical behaviors when assessing their suitability as electrodes in VRFBs. Bearing this in mind, the different felts under evaluation were tested as positive (i.e., vs. VO²⁺/VO₂⁺, information on the proposed mechanism detailed in Figure A1a, Appendix A) and negative (i.e., vs. V³⁺/V²⁺, information on the proposed mechanism detailed in Figure A1b, Appendix A) electrodes, performing the corresponding CV measurements. The resulting electrochemical data, in terms of current densities (j_{pa} , j_{pc}) and potentials of the anodic/cathodic peaks (E_{pa} , E_{pc}), and peak potentials separation values (ΔE_p), were listed in corresponding Tables.

As expected, the raw material (GF) shows a very poor performance towards VO²⁺/VO₂⁺ reaction, as shown in Figure 5. The oxidation process shows a clear peak with a maximum at 1.47 V and a current density of 87.4 mA cm⁻² (Table 1). Nevertheless, the main problem arises from the lack of a well-defined peak associated with the reduction process and the low current density measured, which allows for the inference that the fibre surface is not adequate to promote the redox reaction of the vanadium species, probably because of the poor wettability of the felt due to the low oxygen content.

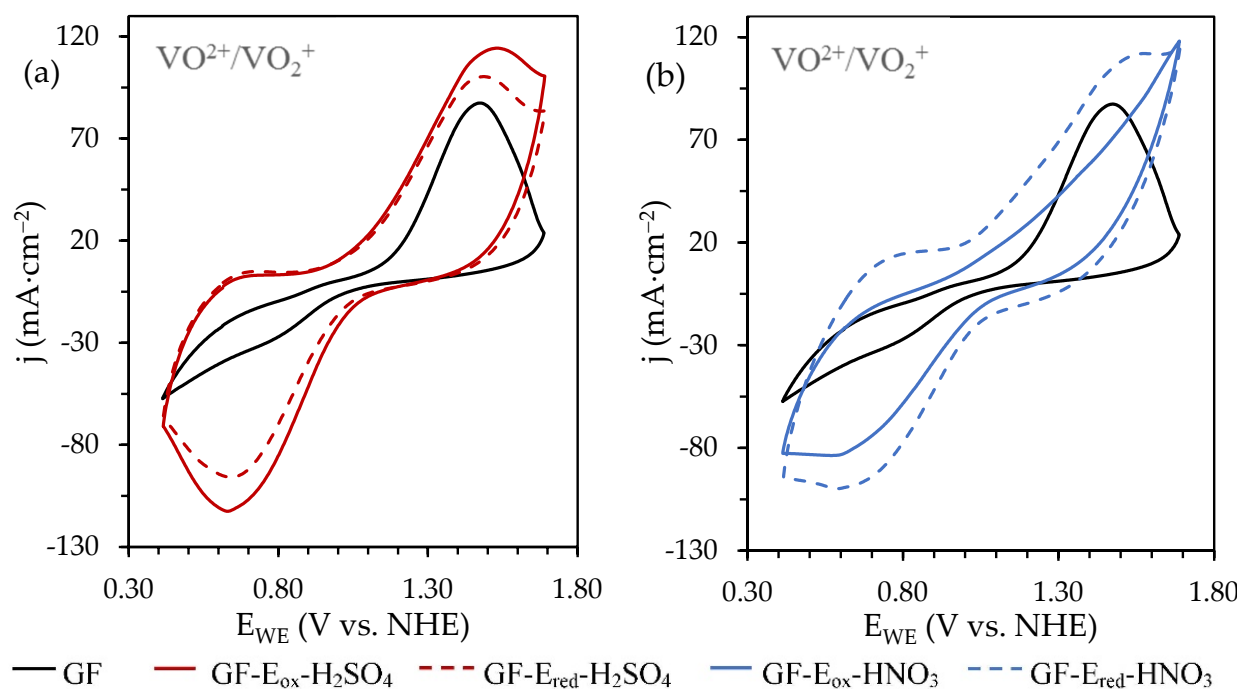


Figure 5. CVs recorded, at 50 mVs^{-1} and towards positive potential values, on the felts electrochemically oxidized and reduced in 1.0 M (a) H_2SO_4 and (b) HNO_3 solutions with 0.05M VOSO_4 /1.0M H_2SO_4 as electrolyte. CVs corresponding to the starting material (GF) were also included for comparative purposes.

Table 1. Electrochemical data derived from CVs recorded, at 50 mVs^{-1} , on the electrodes under evaluation for the $\text{VO}^{2+}/\text{VO}_2^+$ redox pair.

Sample	j_{pa} ($\text{mA} \cdot \text{cm}^{-2}$)	j_{pc} ($\text{mA} \cdot \text{cm}^{-2}$)	$j_{\text{pa}}/j_{\text{pc}}$	$E_{\text{pa}}(\text{V})$	$E_{\text{pc}}(\text{V})$	$\Delta E_{\text{P}}(\text{V})$
GF	87.41	-	-	1.47	0.40	>1.07
GF-E _{ox} - H_2SO_4	114.26	-112.47	1.02	1.53	0.63	0.91
GF-E _{red} - H_2SO_4	100.34	-95.74	1.05	1.49	0.64	0.85
GF-E _{ox} - HNO_3	-	-83.66	-	>1.70	0.57	>1.13
GF-E _{red} - HNO_3	112.01	-99.81	1.12	1.58	0.59	0.99

After electro-oxidation of pristine GF in H_2SO_4 (Figure 5a), the electrochemical activity of GF-E_{ox}- H_2SO_4 improves significantly, showing both an increase of the j_{pa} value (around 35% compared to GF) at a lower overpotential and, more importantly, a well-developed cathodic peak in the reverse scan, reaching a $j_{\text{pa}}/j_{\text{pc}}$ ratio close to the unit (Table 1). These results agree with previously reported ones [31], corroborating the benefit of increasing the oxygen content and, consequently, the amount of OFGs on the surface of the fibres, on improving electrochemical behavior of the modified felt towards $\text{VO}^{2+}/\text{VO}_2^+$. The subsequent electro-reduced GF-E_{red}- H_2SO_4 displays a similar electrochemical trend, although with slight changes. It should be remembered that although during electrooxidation in sulphuric acid the oxygen content increases significantly (from 0.05 to 0.93 wt.% in the fibers bulk and from 2.4 to 15 at.% on the fibers' surface (Tables A1 and A2 Appendix A)), after reduction treatment there are no substantial variations on the oxygen content, which is consistent with the maintenance of the electrochemical behaviour. However, as can be seen, both j_{pa} and j_{pc} are smaller than previously measured on GF-E_{ox}- H_2SO_4 , which could be related to the lower amount of electroactive sites available, as mostly, COOH groups have been removed.

In contrast, the scenario significantly changes when assessing the electrochemical behavior of the felt treated in HNO_3 solution (Figure 5b). The oxidized felt, GF-E_{ox}- HNO_3 ,

displays a very poor performance, particularly towards the VO^{2+} oxidation, showing a badly defined anodic peak. The reason for such behaviour cannot be found in the lack of wettability, as both the oxygen content in the bulk is threefold higher (3.09 wt.%) than the corresponding samples oxidized in sulphuric acid media (Figure 1a), and the surface content increases up to 20 at.% (Tables A1 and A2 Appendix A). Considering previously discussed data, when assessing the chemical composition of the different felts, the poor electro-activity displayed by the GF-E_{ox}-HNO₃ electrode could be explained from two key points, starting from the type of OFGs developed during the electro-oxidation step. The higher amount of carbonyl groups developed under these severe oxidizing conditions seems to have a negative effect on the appropriate development of the $\text{VO}^{2+}/\text{VO}_2^+$ processes, perhaps avoiding a successful access of the redox species to the active sites and worsening the electron-transfer step [32].

However, this unfavourable electrode performance is markedly improved after the subsequent electro-reduction step. As previously stated, the total oxygen content is reduced from 3.09 to 1.14 wt.% (Table A1 Appendix A), which implies that around 63% of the OFGs have been removed, mainly the C=O groups. Furthermore, the Csp² network is markedly restored (up to a 46.8 at.%, Table A2 Appendix A), which seems to facilitate chemical adsorption and to boost the electron-transfer processes. As a result, GF-E_{red}-HNO₃ achieves an electrochemical performance comparable to that of GF-E_{red}-H₂SO₄.

In addition to these surface chemistry observations, the second key point explaining the results recorded on the felts treated in HNO₃ is related to the distribution of OFGs, since they are not only developed on the surface of the fibres, but can also affect their inner structure. In Figure 1, it can be seen that despite exhibiting a similar surface oxygen content, the felt electro-oxidized in H₂SO₄, GF-E_{ox}-HNO₃ has a markedly higher total oxygen content as determined by elemental analysis. Therefore, this fact could be taken as a probe of more aggressive oxidation in nitric acid, affecting not only to the surface (as it seems to be in sulphuric media) but also to the inner structure of the fibres. To support this hypothesis, some measurements were carried out by means of an energy dispersive X-ray analyser (EDX) coupled to a scanning electron microscope (see experimental section) that allows local measurements of the amount of oxygen from the surface of the fibers to their inner structure (Table 2).

Table 2. Carbon and oxygen contents (wt.%) measured from the surface (point 1) to the inner structure of the fibers (points 2 to 5) for pristine GF and felts electrooxidized in different acid media.

Point	Distance ¹ (μm)	GF		GF-E _{ox} -H ₂ SO ₄		GF-E _{ox} -HNO ₃	
		C (wt.%)	O (wt.%)	C (wt.%)	O (wt.%)	C (wt.%)	O (wt.%)
1	0	98.72	1.28	93.67	6.33	94.59	5.41
2	0.3	98.75	1.25	98.76	1.24	96.54	3.46
3	0.6	98.99	1.01	98.64	1.36	96.85	3.15
4	0.9	98.95	1.05	98.73	1.27	98.80	1.20
5	1.2.	99.03	0.97	98.63	1.37	99.02	0.98

¹ Distance measured taking the surface of the fibers as starting point.

The results measured on GF-E_{ox}-H₂SO₄ clearly show that oxygen functionalities are basically restricted to the surface of the fiber, as at 0.3 microns from the surface the O wt.% displays a marked decrease (from 6.33 to 1.24 wt.%), which is in agreement with an electro-oxidation limited to the outer part of the fibres. Contrary to this, results from GF-E_{ox}-HNO₃, show higher oxygen contents at points 2 and 3 than GF (3.46 and 3.15 wt.%, respectively), reflecting oxygen diffusion into the fibre, developing an oxidation layer of around 0.6 μm in thickness from the surface. Hence, it can be inferred that not only the type of OFGs (mainly C=O according to XPS results) but also the depth of the oxidation film is deleterious for the electrochemical performance, influencing both the redox species/active sites contact and the electron transfer step associated to the redox processes of interest.

Carrying on with electrochemical characterization of the different felts, they were also tested as negative electrodes in a VRFB (Figure 6). Differing from previous results related to the faradaic reactions from the catholyte, for the V^{3+}/V^{2+} redox process there are no pronounced differences between oxidized and reduced felts, particularly when assessing those modified in HNO_3 . This fact could be explained considering that the potential window where these vanadium faradaic reactions are developed is the same as that selected for electro-reduction treatments previously described (i.e., the removal of OFGs happens simultaneously). The electrochemical data derived from the corresponding CV experiments are listed in Table 3. According to the results, only the pristine felt offers a poor electrochemical performance and among the modified ones only slight changes can be observed, mainly when considering overpotential values which occur lower on the GF- E_{red} - HNO_3 electrode. The improved behaviour of modified materials can be related to the increase of OFGs, which offer a higher amount of available sites for a suitable development of redox reactions of interest and enhance their wettability in aqueous media (Figure A2, Appendix A). Finally, when comparing the redox activity of different modified felts, it can be seen that the sulphuric acid electro-oxidized electrode shows the best performance, mainly due to their better reversibility.

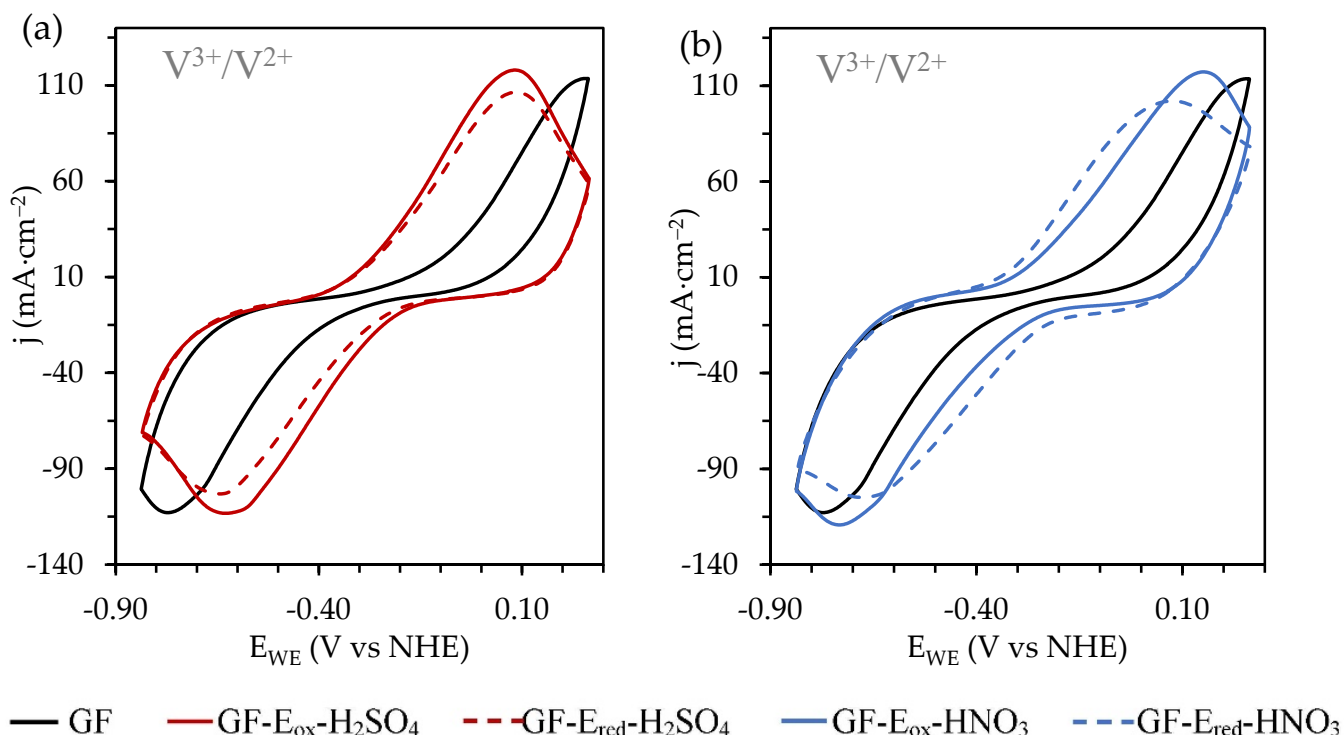


Figure 6. CVs recorded, at 50 mVs^{-1} and towards negative potential values, on the felts electrochemically oxidized and reduced in 1.0 M (a) H_2SO_4 and (b) HNO_3 solutions with 0.05M $VOSO_4/1.0\text{M}$ H_2SO_4 as electrolyte. CVs corresponding to the starting material (GF) were also included for comparative purposes.

Table 3. Electrochemical data derived from CVs recorded, at 50 mVs^{-1} on the electrodes under evaluation, for the V^{3+}/V^{2+} redox pair.

Sample	j_{pa} ($\text{mA}\cdot\text{cm}^{-2}$)	j_{pc} ($\text{mA}\cdot\text{cm}^{-2}$)	j_{pa}/j_{pc}	$E_{pa}(\text{V})$	$E_{pc}(\text{V})$	$\Delta E_p(\text{V})$
GF	113.63	-112.87	1.01	0.26	-0.77	1.04
GF-E _{ox} - H_2SO_4	118.01	-113.21	1.04	0.09	-0.63	0.72
GF-E _{red} - H_2SO_4	106.45	-103.05	1.03	0.09	-0.65	0.74
GF-E _{ox} - HNO_3	117.23	-119.28	0.98	0.16	-0.74	0.89
GF-E _{red} - HNO_3	102.01	-104.94	0.97	0.08	-0.68	0.76

Finally, EIS experiments were performed to elucidate in depth the impact of the chemical composition of the different felts on charge transfer and diffusion steps involved in vanadium redox reactions from both catholyte and anolyte. An optimized equivalent circuit was inferred by fitting the impedance data from EIS measurements (Figure 7, Tables A3 and A4, Appendix A) [33,34].

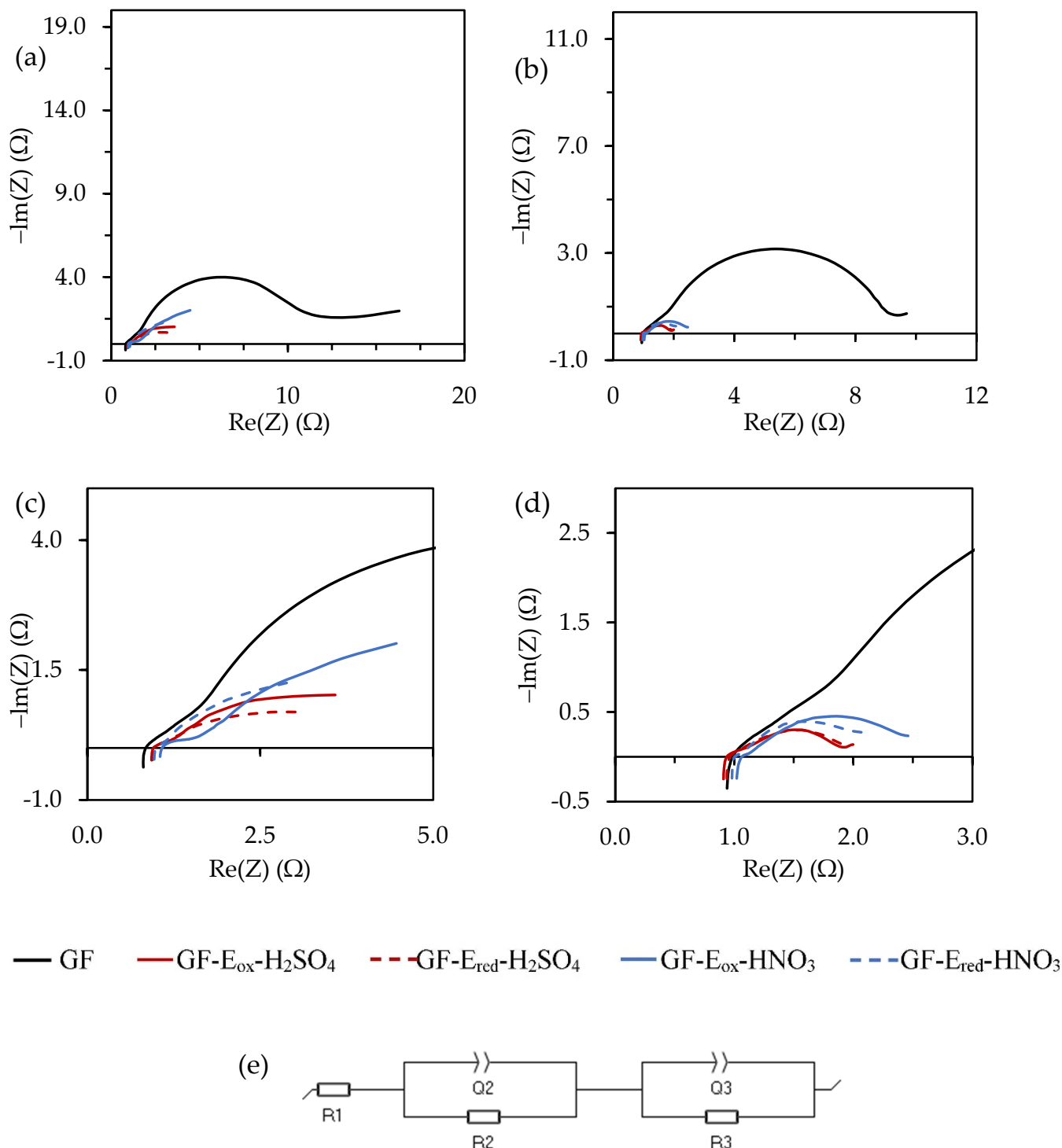


Figure 7. Nyquist plots from the different felts in 0.05 M VOSO₄/1.0 M H₂SO₄ at 1.1 (vs. VO²⁺/VO₂⁺) (a) and −0.3 (vs. V³⁺/V²⁺) V (b). (c,d) magnification of the high frequency range of (a,b), respectively. The equivalent circuit selected to fit the impedance data (e).

Even though samples under study show quite different behaviour, R_1 values, mainly related to the resistance of the electrolyte (and electrolyte/electrode contact resistance), are very similar for all the plots (data summarized in Tables A3 and A4).

Analyzing the plots recorded on each felt, GF shows the expected behaviour, with two well-defined semicircles at high and low frequency regions that can be attributed to the formation of the double layer and to the resistance associated to the charge transfer step, respectively. Due to the negligible specific surface area and poor wettability in aqueous media of this material, the Q_2 value is significantly low when compared to the modified felts. However, most importantly, its high resistance to charge transfer step (R_3) and the very low value of Q_3 are remarkable, reflecting that vanadium redox reactions occur in a very small extension on this electrode, in agreement with CV results and thus corroborating its unsuitability as active electrode material.

Regarding the modified felts, important differences can be observed in the medium-high frequency region. R_2 is associated to the double layer formation and to the electrical resistance of the cell set up, including current collector/electrode contact, these values being very small, although higher values were found for GF-E_{ox}-HNO₃, confirming that the electrochemical procedures undergone affect the electrical conductivity of these felts. In the low frequency region, the second semicircle, associated with the resistance of the charge transfer step during the redox reaction, is noticeably larger for the GF-E_{ox}-HNO₃, clearly indicating that this step is impeded on this electrode and thus corroborating previously discussed CV results. Indeed, these results could perfectly correlate with the presence of a thicker layer enriched in oxygen functionalities, mainly carbonyl groups, hindering the redox processes of interest.

The results obtained for the negative electrode (Figure 7b,d) show smaller differences as the redox reactions involved occur smoothly and are less dependent on the surface functionalities. Nevertheless, slight differences found point in the same direction, with GF-E_{ox}-HNO₃ being more resistive.

3. Materials and Methods

Preparation of electrodes by electrochemical treatments: The raw material used was a polyacrylonitrile (PAN)-based graphite felt (GF, Sigracell GFD 4.65 EA from SGL Carbon, Germany).

The electro-oxidation treatments were performed in a lab-made cell (Figure A3 Appendix A), at room temperature, using a Biologic VMP Multichannel Potentiostat workstation (Biologic, Seyssinet-Pariset, France) equipped with a booster of 10 A/20 V. 80 mL of 1.0 M H₂SO₄ (VWR International Eurolab SLU, Barcelona, Spain) or 1.0 M HNO₃ 1 M (Sigma-Aldrich, Darmstadt, Germany) solutions were used as electrolyte for the anodic oxidation of graphite felts. Two portions of the as received GF (6 × 6 cm²), each one compressed between two graphite frames leaving an exposed geometric surface of 25 cm², were placed maintaining a distance of 2 cm between them, one acting as working electrode (WE) and the other one as counter electrode (CE), and immersed into the corresponding acid solution. In addition, an Ag/AgCl/3.5 M KCl (i.e., 0.214 V vs. NHE) reference electrode (RE) was placed between them. All of the potential values were referenced to the normal hydrogen electrode (NHE).

In the first stage, the felts were oxidized by applying to the WE a fixed current density (d_c) of 200 mA·cm⁻² which is equivalent to a specific charge per mass unit (C_{spec}) of 5000 C·g⁻¹. The corresponding applied current (I) and time of treatment (t) were calculated from Equations (1) and (2), considering the mass and the geometric surface of the piece of felt (m_{felt} and S_{felt} , respectively) (Table 4). The oxidized felts were labelled as GF-E_{ox}-H₂SO₄ and GF-E_{ox}-HNO₃, according to the electrolyte used.

$$I(\text{mA}) = d_c(\text{mA} \cdot \text{cm}^{-2}) \cdot S_{\text{felt}}(\text{cm}^2) \quad (1)$$

$$t(\text{s}) = (C_{\text{spec}}(\text{C} \cdot \text{g}^{-1}) \cdot m_{\text{felt}}(\text{g}) \cdot 1000) / I(\text{mA}) \quad (2)$$

Table 4. Specifications and electrochemical parameters derived from Equations (1) and (2) for electro-oxidation treatment.

Sample	Electrolyte	m_{felt} (g)	S_{felt} (cm^2)	d_c ($\text{mA} \cdot \text{cm}^2$)	I (mA)	C_{spec} ($\text{C} \cdot \text{g}^{-1}$)	t (s)
GF-E _{ox} -H ₂ SO ₄	1.0 M H ₂ SO ₄	1.663	25	200	5000	5000	1663
GF-E _{ox} -HNO ₃	1.0 M HNO ₃	1.648	25	200	5000	5000	1648

In a second stage, some of the previously electro-oxidized felts were then subjected to an electrochemical reduction step. For this purpose, the same cell and electrolyte were used and a CV experiment was carried out between 0.089 and -0.686 V (10 repetitive scans at $20 \text{ mV} \cdot \text{s}^{-1}$). The reduced felts were labelled as GF-E_{red}-H₂SO₄ and GF-E_{red}-HNO₃. After the different treatments were performed, the resulting materials were neutralised with milli-Q water and dried overnight before being used (90°C , vacuum conditions).

Characterization of electro-oxidized and electro-reduced felts: The characteristics of the felts submitted to different electrochemical treatments were carefully examined and compared to those of the starting materials. The bulk oxygen was determined directly in a LECO VTF-900 (Leco Instrumentos S.L., Madrid, Spain) furnace coupled to a LECO-CHNS-932 microanalyzer. The morphology of the modified felts (Figure A4, Appendix A) and profiles of oxygen content (wt.%) distribution from the surface to the inner of the electrooxidized fibres were assessed by Scanning electron microscopy (SEM) fitted with an energy dispersive X-ray analyser (EDX). SEM measurements (MEB JEOL-6610LV instrument, FEI, Czech Republic, operating at 5 kV) were performed on randomly selected felt pieces and EDX (INCA ENERGY350-Xmax 50) was fitted to allow the detection and quantification of the oxygen present in selected points. The atomic surface oxygen content (at.%) was measured by X-ray photoelectron spectroscopy (XPS) analysis in a VG-Microtech Multilab 3000 spectrometer (SPECS, Berlin, Germany) equipped with a hemispherical electron analyser and a MgK α ($h\nu = 1253.6$ eV) X-ray source. The type of bonding and the functional groups present in the samples were estimated by curve fitting the C1s spectra using a Gaussian–Lorentzian peak shape after performing a Shirley background correction [35]. The binding energy profiles were deconvoluted as follows: the main peak at 284.5 eV was assigned to C-C sp² and the other four peaks were attributed to C-C sp³ (285.0–285.3 eV), C-OH (286.1–286.5 eV), C=O (287.0–287.5 eV), COOH functional groups (288.5–289.0 eV) and π - π^* (290.9–291.2 eV). In order to estimate a reliable value of the percentages corresponding to each functional group, thus allowing an appropriate comparison of the samples, all the values derived from the deconvolution were corrected considering the atomic-specific content of C1s (%) for each sample. Equation (3) gives an example of the calculation made regarding the Csp² content.

$$C_{\text{sp}}^2 (\%) = A_{\text{Csp}}^2 \text{ fitting} (\%) \cdot C_{1s} (\text{at.}\%) / 100 \quad (3)$$

Electrochemical characterization of felts: The electrochemical characterization of the different felts under evaluation was performed in a Teflon® home-made three-electrode cell (detailed design on Appendix A, Figure A5a [36]) at room temperature using a Biologic VMP Multichannel Potentiostat workstation (Biologic, France). Coin-type portions of the pristine and modified felts (geometric surface of 2.0 cm^2) acted as WEs, while Ag/AgCl/3.5 M KCl (i.e., 0.214 V vs. NHE) and a graphite rod were used as RE and CE, respectively. The three electrodes setup is detailed in Appendix A, Figure A5b. The WEs were compressed, up to a compression percentage value of 75%, between the graphite disk used as a current collector and a Teflon sheet with a hole of 11 mm in diameter allowing the electroactive species accessing the working electrode. CV experiments were carried out in a 0.05 M VOSO₄ (Sigma Aldrich, Germany)/1.0 M H₂SO₄ (VWR International Eurolab SLU, Spain) solution of between 0.3–1.8 V and -0.9 – -0.6 V (vs. NHE) to evaluate the suitability of the modified felts towards the VO²⁺/VO₂⁺ and V³⁺/V²⁺ processes, respectively, with a scan rate of $50 \text{ mV} \cdot \text{s}^{-1}$. Electrochemical impedance spectroscopy (EIS) measurements were carried out in the same electrolytes fixing polarization potentials of 1.1 and -0.3 V (vs. NHE), to check

both $\text{VO}^{2+}/\text{VO}_2^+$ and the $\text{V}^{3+}/\text{V}^{2+}$ redox reactions, respectively, at an amplitude of 10 mV over a frequency range of 100 kHz to 500 mHz.

4. Conclusions

The in-depth analysis of various oxidized graphite felts carried out in this work enabled the understanding of key issues influencing the improvement of their electrochemical behavior towards faradaic processes related to electroactive vanadium species. Not only are the amount of oxygen incorporated or the type of OFGs developed crucial, but so are the thickness of the oxidation layer achieved on the fibres. The latter is an important parameter, as it can alter the electrical conductivity of the fibre and, subsequently, the charge transfer step related to the redox reactions occurring in the battery, but the study of its influence is usually neglected.

A moderate electro-oxidation treatment in sulphuric acid provides the adequate OFGs type (mainly –OH and –COOH) and proportion to achieve the best electrochemical performance on VRFBs. A slight increment of the oxygen content has a positive impact not only in the improvement of the wettability of the felt, but also has a relevant role on its electrochemical behaviour, providing available and stable active sites that promote the kinetics of the anodic/cathodic redox processes and facilitate the electron and oxygen atom transfer for the vanadium ions.

On the other hand, aggressive electro-oxidation in nitric acid drives an important decrease in the performance of the felts as positive electrodes due to the formation of a thick oxidized layer (around 0.6 µm) that difficult the electron transfer step and the access of the electroactive species to the active sites. This thick layer, mainly formed by carbonyl groups, is readily reduced when the felt underwent negative reduction potentials.

Author Contributions: L.G.-A.: Conceptualization, Methodology, Investigation, Writing—original draft. A.C.: Conceptualization, Methodology, Investigation. V.G.R.: Conceptualization, Writing—review & editing. C.B.: Conceptualization, Supervision, Writing—review & editing, Funding acquisition. R.S.: Conceptualization, Supervision, Writing—review & editing, Funding acquisition, Project administration. Z.G.: Conceptualization, Methodology, Supervision, Writing—review & editing. All authors have read and agreed to the published version of the manuscript.

Funding: Ricardo Santamaría and Clara Blanco report financial support provided by the CSIC program for the Spanish Recovery, Transformation and Resilience Plan funded by the Recovery and Resilience Facility of the European Union, established by the Regulation (EU) 2020/2094 (TRE2103001). Moreover, Ricardo Santamaría also reports financial support provided by the Spanish Research Agency (AEI/PID2019-104028RB-100). Clara Blanco reports financial support provided by Principado de Asturias (FICYT, Ayudas a grupos de investigación para actividades de I+D+i 2021-2023, AYUD/2021/50249). Victoria G. Rocha reports financial support provided by the Spanish Government (Ramón y Cajal fellowship, RYC2018-024404-I).

Institutional Review Board Statement: Not applicable.

Informed Consent Statement: Not applicable.

Data Availability Statement: Not applicable.

Acknowledgments: This research (in the framework of PTI+ TRANSENER, Sustainable Energy Transition) is part of the CSIC program for the Spanish Recovery, Transformation and Resilience Plan funded by the Recovery and Resilience Facility of the European Union, established by the Regulation (EU) 2020/2094 (TRE2103001). Authors would also thank the Spanish Research Agency (AEI/PID2019-104028RB-100) and Principado de Asturias (FICYT, Ayudas a grupos de investigación para actividades de I+D+i 2021-2023, AYUD/2021/50249) for its financial support. V. G. Rocha would like to thank the Spanish Government (Ramón y Cajal fellowship, RYC2018-024404-I).

Conflicts of Interest: The authors declare that they have no conflict of interest.

Appendix A

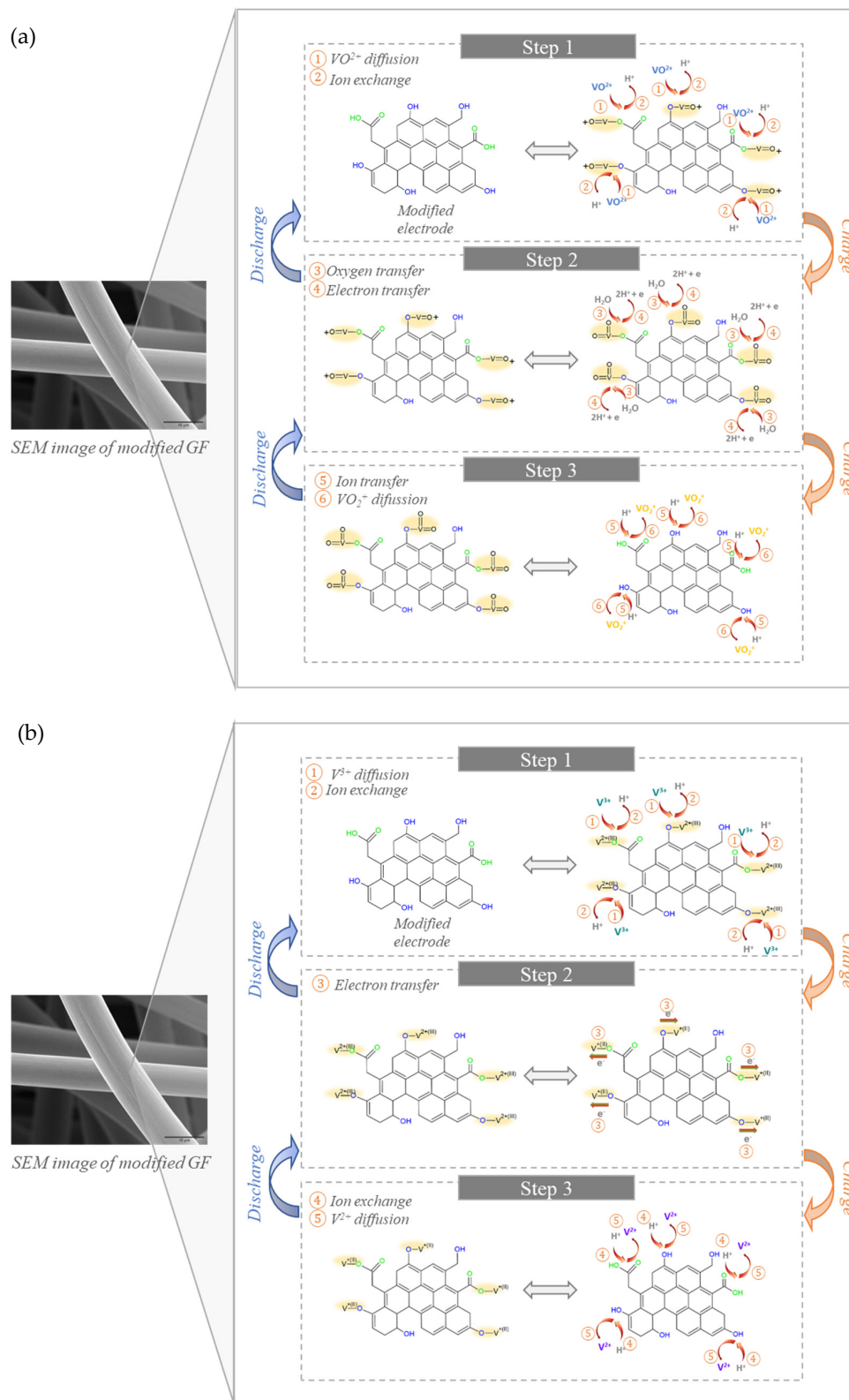


Figure A1. Schematic representation of the mechanisms proposed for the reaction of the modified felts towards the faradaic processes involving the vanadium species present on the positive (a) and negative (b) half-cells.

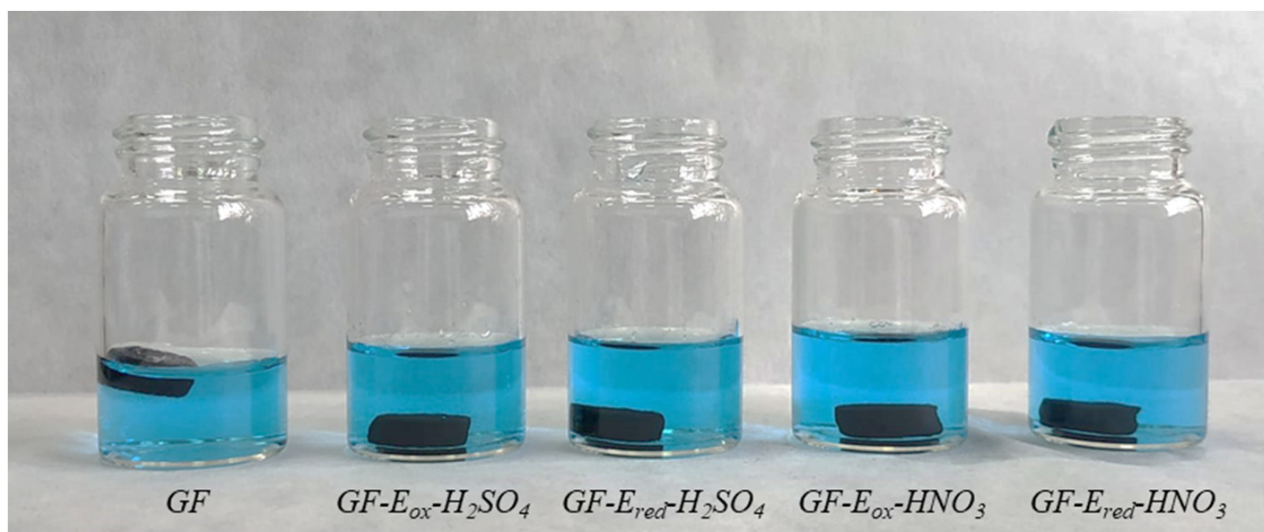


Figure A2. Image showing the enhanced wettability of the modified felts when immersed in the vanadium-based electrolyte.

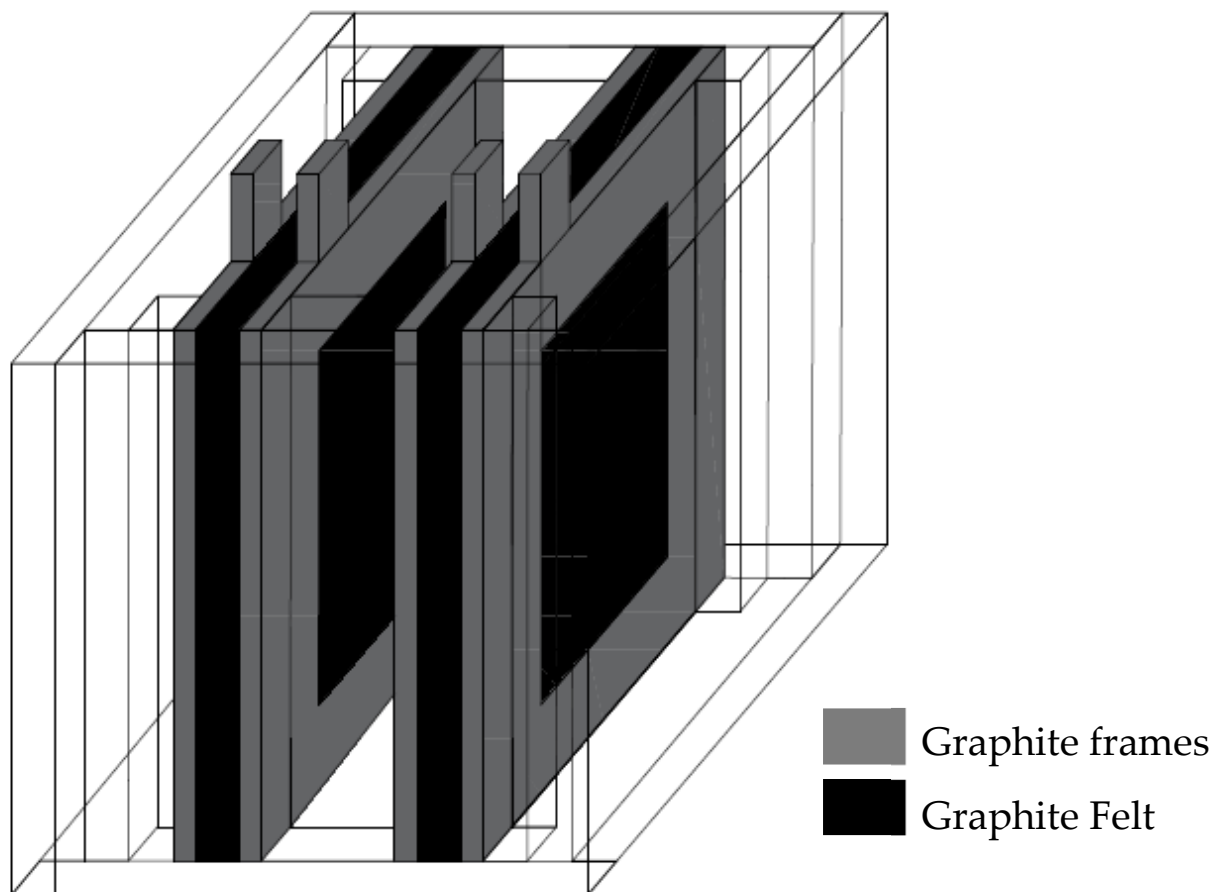


Figure A3. Schematic representation of the custom-made electrochemical cell employed for performing the electro-oxidation and electro-reduction treatments.

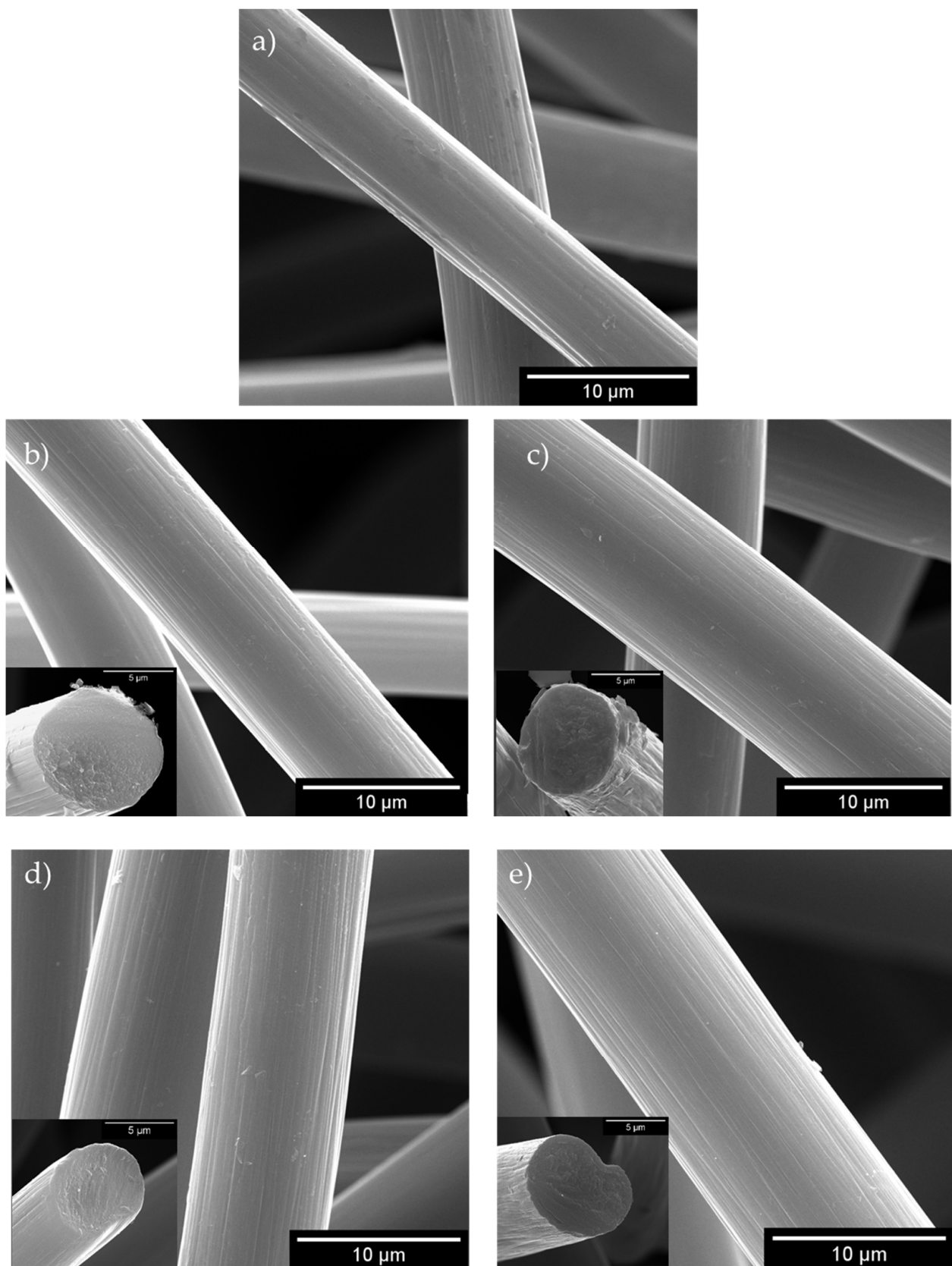


Figure A4. SEM images of the starting GF (a), GF-E_{ox}-H₂SO₄ (b), GF-E_{ox}-HNO₃ (c), GF-E_{red}-H₂SO₄ (d) and GF-E_{red}-HNO₃ (e). Insertions in (b–e) present cross-sectional views of the corresponding modified fibres.

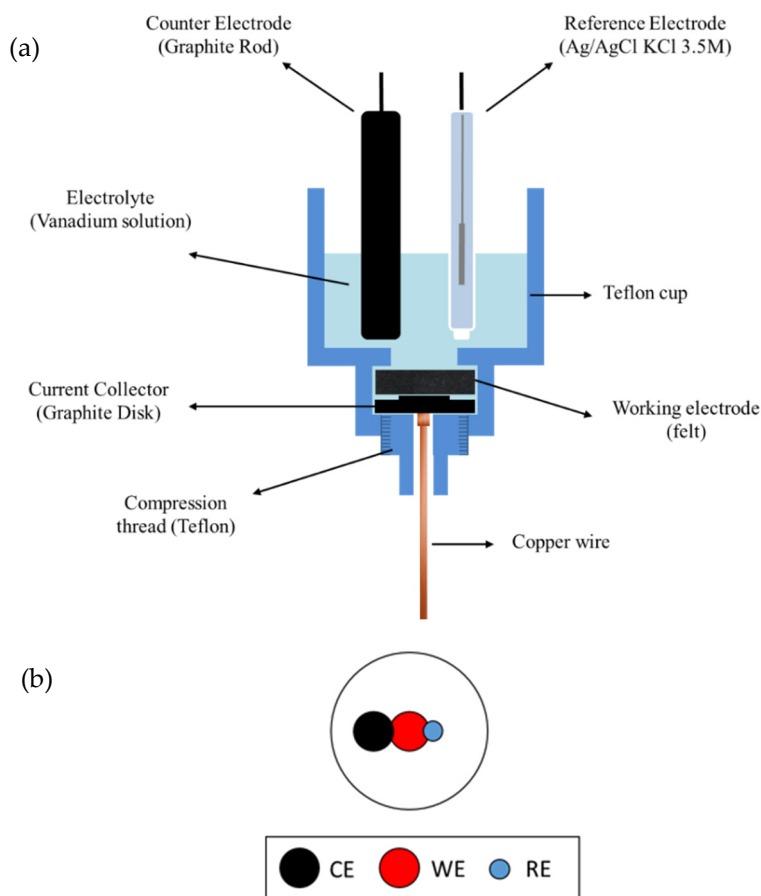


Figure A5. Scheme of the Teflon® lab-made 3-electrode set up (a) and electrodes relative configuration (b) selected for carrying out the electrochemical characterization of the felts under evaluation. Reprinted with permission from Ref. [36]. 2022, Elsevier.

Table A1. Results from elemental microanalysis of pristine and modified graphite felts.

Sample	Elemental Composition (wt.%)		
	C	H	O
GF	99.86	0.01	0.05
GF-E _{ox} -H ₂ SO ₄	98.29	0.10	0.93
GF-E _{red} -H ₂ SO ₄	97.54	0.40	1.08
GF-E _{ox} -HNO ₃	96.00	0.25	3.09
GF-E _{red} -HNO ₃	98.11	0.08	1.14

Table A2. Surface chemistry of the starting and electrochemically treated graphite felts.

Sample	Csp ² (%)	Csp ³ (%)	C-OH (%)	C=O (%)	COOH (%)	π-π* (%)	C (at. %)	O (at. %)
GF	56.8	24.0	6.7	2.4	2.2	5.4	97.4	2.4
GF-E _{ox} -H ₂ SO ₄	34.1	26.0	10.2	4.7	7.9	1.6	84.5	15.0
GF-E _{red} -H ₂ SO ₄	38.9	26.9	10.7	3.4	5.2	2.6	87.6	12.0
GF-E _{ox} -HNO ₃	21.9	22.8	10.9	18.4	5.1	0.7	79.9	20.0
GF-E _{red} -HNO ₃	46.8	22.3	8.5	1.0	8.5	2.2	89.3	10.2

Table A3. Impedance data derived from the Nyquist plots (Figure 7a) recorded on the different felts at a potential of 1.1 V (vs. $\text{VO}^{2+}/\text{VO}_2^+$).

Equivalent Circuit	R_1 (Ω)	Q2/R2			Q3/R3		
		Sample	$R_2(\Omega)$	$Q_2(\text{F}\cdot\text{s}^{n-1})$	n_2	$R_3(\Omega)$	$Q_3(\text{F}\cdot\text{s}^{n-1})$
GF	0.84	0.74	7.78×10^{-3}	0.69	10.27	7.49×10^{-3}	0.86
GF-E _{ox} -H ₂ SO ₄	0.95	0.29	0.049	0.66	3.48	0.262	0.70
GF-E _{red} -H ₂ SO ₄	0.96	0.19	0.052	0.70	2.57	0.232	0.63
GF-E _{ox} -HNO ₃	1.07	0.51	0.023	0.62	6.95	0.293	0.65
GF-E _{red} -HNO ₃	0.99	0.09	0.167	0.69	4.06	0.393	0.70

Table A4. Impedance data derived from the Nyquist plots (Figure 7b) recorded on the different felts at and at a potential of −0.3 V (vs. $\text{V}^{3+}/\text{V}^{2+}$).

Equivalent Circuit	R_1 (Ω)	Q2/R2			Q3/R3		
		Sample	$R_2(\Omega)$	$Q_2(\text{F}\cdot\text{s}^{n-1})$	n_2	$R_3(\Omega)$	$Q_3(\text{F}\cdot\text{s}^{n-1})$
GF	0.98	0.78	2.65×10^{-3}	0.75	7.42	3.35×10^{-3}	0.88
GF-E _{ox} -H ₂ SO ₄	0.91	0.83	0.33	0.40	0.34	0.17	0.99
GF-E _{red} -H ₂ SO ₄	0.95	0.58	0.17	0.51	0.47	0.12	0.87
GF-E _{ox} -HNO ₃	1.05	0.47	0.68	0.37	1.07	0.17	0.81
GF-E _{red} -HNO ₃	1.00	0.27	0.51	0.52	0.81	0.30	0.92

References

- European Union Energy Roadmap 2050. Available online: https://ec.europa.eu/energy/sites/ener/files/documents/2012_energy_roadmap_2050_en_0.pdf (accessed on 10 May 2022).
- Fetting, C. The European Green Deal, ESDN Report, December 2020, ESDN Office, Vienna. Available online: https://eur-lex.europa.eu/resource.html?uri=cellar:b828d165-1c22-11ea-8c1f-01aa75ed71a1.0002.02/DOC_1&format=PDF (accessed on 12 May 2022).
- Sánchez-Díez, E.; Ventosa, E.; Guarnieri, M.; Trovò, A.; Flox, C.; Marcilla, R.; Soavi, F.; Mazur, P.; Aranzabe, E.; Ferret, R. Redox flow batteries: Status and perspective towards sustainable stationary energy storage. *J. Power Source* **2021**, *481*, 228804. [[CrossRef](#)]
- Pan, F.; Wang, Q. Redox species of redox flow batteries: A review. *Molecules* **2015**, *11*, 20499–20517. [[CrossRef](#)]
- Zhang, H.; Sun, C. Cost-effective iron-based aqueous redox flow batteries for large-scale energy storage application: A review. *J. Power Source* **2021**, *493*, 229445. [[CrossRef](#)]
- Guo, L.; Guo, H.; Huang, H.; Tao, S.; Cheng, Y. Inhibition of zinc dendrites in zinc-based flow batteries. *Front. Chem.* **2020**, *8*, 557. [[CrossRef](#)] [[PubMed](#)]
- Sun, C.; Negro, E.; Nale, A.; Pagot, G.; Vezzù, K.; Zawodzinski, T.A.; Meda, L.; Gambaro, C.; Di Noto, V. An efficient barrier toward vanadium crossover in redox flow batteries: The bilayer [Nafion/(WO₃)_x] hybrid inorganic-organic membrane. *Electrochim. Acta* **2021**, *378*, 138133. [[CrossRef](#)]
- Castañeda, L.F.; Walsh, F.C.; Nava, J.L.; Ponce De Leon, C. Graphite felt as a versatile electrode material: Properties, reaction environment, performance and applications. *Electrochim. Acta* **2017**, *258*, 1115–1139. [[CrossRef](#)]
- Kim, K.J.; Park, M.S.; Kim, Y.J.; Kim, J.H.; Doub, S.X.; Skyllas-Kazacos, M. A technology review of electrodes and reaction mechanisms in vanadium redox flow batteries. *J. Mater. Chem. A* **2015**, *3*, 16913–16933. [[CrossRef](#)]
- He, Z.; Lv, Y.; Zhang, T.; Zhu, Y.; Dai, L.; Yao, S.; Zhu, W.; Wang, L. Electrode materials for vanadium redox flow batteries: Intrinsic treatment and introducing catalyst. *Chem. Eng. J.* **2022**, *427*, 131680. [[CrossRef](#)]
- Radinger, H. 2021: A Surface Odyssey. Role of Oxygen Functional Groups on Activated Carbon-Based Electrodes in Vanadium Flow Batteries. *ChemPhysChem* **2021**, *22*, 2498–2505. [[CrossRef](#)]
- Sun, B.; Skyllas-Kazacos, M. Modification of graphite electrode materials for vanadium redox flow battery application—I. Thermal treatment. *Electrochim. Acta* **1992**, *7*, 1253–1260. [[CrossRef](#)]
- Sun, B.; Skyllas-Kazacos, M. Chemical modification of graphite electrode materials for vanadium redox flow battery application—II Acid treatments. *Electrochim. Acta* **1992**, *13*, 2459–2465. [[CrossRef](#)]
- Kim, K.J.; Kim, Y.J.; Kim, J.H.; Park, M.S. The effects of surface modification on carbon felt electrodes for use in vanadium redox flow batteries. *Mater. Chem. Phys.* **2011**, *131*, 547–553. [[CrossRef](#)]
- Dixon, D.; Babu, D.J.; Langner, J.; Bruns, M.; Pfaffmann, L.; Bhaskara, A.; Schneider, J.J.; Scheiba, F.; Ehrenberg, H. Effect of oxygen plasma treatment on the electrochemical performance of the rayon and polyacrylonitrile based carbon felt for the vanadium redox flow battery application. *J. Power Source* **2016**, *332*, 240–248. [[CrossRef](#)]
- Wu, X.; Xu, H.; Xu, P.; Shen, Y.; Lu, L.; Shi, J.; Fu, J.; Zhao, H. Microwave-treated graphite felt as the positive electrode for all-vanadium redox flow battery. *J. Power Source* **2014**, *263*, 104–109. [[CrossRef](#)]

17. Cho, Y.I.; Park, S.J.; Hwang, H.J.; Lee, J.G.; Jeon, Y.K.; Chu, Y.H.; Shul, Y. Effects of Microwave Treatment on Carbon Electrode for Vanadium Redox Flow Battery. *ChemElectroChem* **2015**, *2*, 872–876. [[CrossRef](#)]
18. Li, W.; Zhang, Z.; Tang, Y.; Bian, H.; Ng, T.; Zhang, W.; Lee, C. Graphene-Nanowall-Decorated Carbon Felt with Excellent Electrochemical Activity Toward $\text{VO}^{2+}/\text{VO}_2^+$ Couple for All Vanadium Redox Flow Battery. *Adv. Sci.* **2016**, *3*, 1500276. [[CrossRef](#)]
19. Etienne, M.; Vivo-Vilches, J.F.; Vakulko, I.; Genois, C.; Liu, L.; Perdicakis, M.; Hempelmann, R.; Walcarius, A. Layer-by-Layer modification of graphite felt with MWCNT for vanadium redox flow battery. *Electrochim. Acta* **2019**, *313*, 131–140. [[CrossRef](#)]
20. Li, X.; Huang, K.-L.; Liu, S.-Q.; Tan, N.; Chen, L.-Q. Characteristics of graphite felt electrode electrochemically oxidized for vanadium redox battery application. *Trans. Nonferrous Met. Soc. China* **2007**, *17*, 195–199. [[CrossRef](#)]
21. Li, X.; Huang, K.-L.; Liu, S.-Q.; Chen, L.-Q. Electrochemical behaviour of diverse vanadium ions at modified graphite felt electrode in sulphuric solution. *J. Cent. South Univ. Technol.* **2007**, *14*, 51–56. [[CrossRef](#)]
22. Zhang, W.; Xi, J.; Li, Z.; Zhoua, H.; Liua, L.; Wu, Z.; Qiu, X. Electrochemical activation of graphite felt electrode for $\text{VO}^{2+}/\text{VO}_2^+$ redox couple application. *Electrochim. Acta* **2013**, *89*, 429–435. [[CrossRef](#)]
23. Wang, W.; Wei, Z.; Su, W.; Fan, X.; Liu, J.; Yan, C.; Zeng, C. Kinetic investigation of vanadium (V)/(IV) redox couple on electrochemically oxidized graphite electrodes. *Electrochim. Acta* **2016**, *205*, 102–112. [[CrossRef](#)]
24. Li, W.; Liu, J.; Yan, C. Reduced graphene oxide with tunable C/O ratio and its activity towards vanadium redox pairs for an all vanadium redox flow battery. *Carbon* **2013**, *55*, 313–320. [[CrossRef](#)]
25. Noack, J.; Roznyatovskaya, N.; Kunzendorf, J.; Skyllas-Kazacos, M.; Menictas, C.; Tübke, J. The influence of electrochemical treatment on electrode reactions for vanadium redox-flow batteries. *J. Energy Chem.* **2018**, *27*, 1341–1352. [[CrossRef](#)]
26. Miller, M.A.; Bourke, A.; Quill, N.; Wainright, J.S.; Lynch, R.P.; Buckley, D.N.; Savenill, R.F. Kinetic study of electrochemical treatment of carbon fiber microelectrodes leading to in situ enhancement of vanadium flow battery efficiency. *J. Electrochem. Soc.* **2016**, *9*, A2095–A2102. [[CrossRef](#)]
27. Taylor, S.M.; Patru, A.; Perego, D.; Fabbri, E.; Schmidt, T.J. Influence of carbon material properties on activity and stability of the negative electrode in vanadium redox flow batteries: A model electrode study. *ACS Appl. Energy Mater.* **2018**, *1*, 1166–1174. [[CrossRef](#)]
28. Kabir, H.; Gyan, I.O.; Cheng, I.F. Electrochemical modification of a pyrolytic graphite sheet for improved negative electrode performance in the vanadium redox flow battery. *J. Power Source* **2017**, *342*, 31–37. [[CrossRef](#)]
29. Bourke, A.; Miller, M.A.; Lynch, R.P.; Gao, X.; Landon, J.; Wainright, J.S.; Savinell, R.F.; Buckley, D.N. Electrode kinetics of vanadium flow batteries: Contrasting responses of V(II)-V(III) and V(IV)-V(V) to electrochemical pre-treatment of carbon. *J. Electrochem. Soc.* **2016**, *1*, A5097–A5105. [[CrossRef](#)]
30. Xi, J.; Zhang, W.; Li, Z.; Zhou, H.; Liu, L.; Wu, Z.; Qiu, X. Effect of electro-oxidation current density on performance of graphite felt electrode for vanadium redox flow battery. *Int. J. Electrochem. Sci.* **2013**, *8*, 4700–4711.
31. García-Alcalde, L.; González, Z.; Barreda, D.; García-Rocha, V.; Blanco, C.; Santamaría, R. Unraveling the relevance of carbon felts surface modification during electrophoretic deposition of nanocarbons on their performance as electrodes for the $\text{VO}^{2+}/\text{VO}_2^+$ redox couple. *Appl. Surf. Sci.* **2021**, *569*, 151095. [[CrossRef](#)]
32. McCreery, R.L.; Cline, K.K.; McDermott, C.A.; McDermott, M.T. Control of reactivity at carbon electrode surfaces. *Colloids Surf. A Physicochem. Eng. Asp.* **1994**, *93*, 211–219. [[CrossRef](#)]
33. Wang, W.H.; Wang, X.D. Investigation of Ir-modified carbon felt as the positive electrode of an all-vanadium redox flow battery. *Electrochim. Acta* **2007**, *52*, 6755–6762. [[CrossRef](#)]
34. Yue, L.; Li, W.; Sun, F.; Zhao, L.; Xing, L. Highly hydroxylated carbon fibres as electrode materials of all-vanadium redox flow battery. *Carbon* **2010**, *48*, 3079–3090. [[CrossRef](#)]
35. Sherwood, P.M.A. *Practical Surface Analysis, Auger and X-ray Photoelectron Spectroscopy*; Briggs, D., Seah, M.P., Eds.; Wiley: New York, NY, USA, 1990; Volume 1, p. 574.
36. García-Alcalde, L.; González, Z.; Concheso, A.; Blanco, C.; Santamaría, R. Impact of electrochemical cells configuration on a reliable assessment of active electrode materials for vanadium redox flow batteries. *Electrochim. Acta* **2022**, *432*, 141225. [[CrossRef](#)]